Determining time resolution of microchannel plate detectors for electron time-of-flight spectrometers

Qi Zhang (张琦),[1] Kun Zhao (赵昆),[1] and Zenghu Chang (常增虎)[1,2,a)]
[1]*J.R. Macdonald Laboratory, Department of Physics, Kansas State University, Manhattan, Kansas 66506, USA*
[2]*Department of Physics and CREOL, University of Central Florida, Orlando, Florida 32816, USA*

(Received 23 February 2010; accepted 22 June 2010; published online 28 July 2010)

The temporal resolution of a 40 mm diameter chevron microchannel plate (MCP) detector followed by a constant fraction discriminator and a time-to-digital converter was determined by using the third order harmonic of 25 fs Ti:sapphire laser pulses. The resolution was found to deteriorate from 200 to 300 ps as the total voltage applied on the two MCPs increased from 1600 to 2000 V. This was likely due to a partial saturation of the MCP and/or the constant fraction discriminator working with signals beyond its optimum range of pulse width and shape. © *2010 American Institute of Physics.* [doi:10.1063/1.3463690]

I. INTRODUCTION

Extreme ultraviolet (XUV) attosecond pulses are usually characterized with an attosecond streak camera, where the XUV pulses are converted to their electron replica first through photoionization of atoms. The electron spectrum is then modified by a strong near infrared (NIR) laser field. The XUV pulse shape and phase are retrieved from the streaked photoelectron energy spectra.[1–3] Time-of-flight (TOF) spectrometers are used for such electron energy spectrum measurement. An XUV pulse of 25 as, which is about one atomic unit of time, corresponds to a photoelectron spectrum of 75 eV full-width-at-half-maximum (FWHM), which requires the spectrometer to cover a ~200 eV energy range. To resolve pre- or postpulses one NIR laser cycle away from the main pulse, the resolution of the spectrometer should be better than 0.5 eV in the whole energy range.[4] It is also critical to detect as many electrons as possible in attosecond photoelectron measurements due to the low XUV photon flux and low XUV to electron conversion efficiency. Constructing such a TOF spectrometer is a challenging task.

To that end, a magnetic-bottle electron TOF energy spectrometer (MBEES) is under development for such measurements. The nonuniform magnetic field in MBEES ensures the acceptance angle of the detector is larger than 2π sr.[5,6] The energy resolution of a TOF spectrometer depends on the length of the flight tube and the temporal resolution of the electron detection system. A flight tube longer than 3 m is not convenient to use. To achieve the needed resolution of 0.5 eV, even for such a long tube, our simulation shows that a temporal resolution of 250 ps or better is required for the microchannel plate (MCP) electron detector and the data acquisition (DAQ) electronic system including fast amplifier, constant-fraction discriminator (CFD), and time-to-digital converter (TDC).

Determination of the temporal resolution of the MCP and DAQ is difficult because of the lack of electron pulses much shorter than the time resolution. In previous studies, a variety of particles have been employed to characterize MCP-based detectors, including a synchrotron ion beam,[7] Linac electron beam,[8] 200 ps pulsed electron source,[9] and photons from a synchrotron (50–100 ps FWHM)[10,11] as well as from visible or UV lasers with pulse widths (FWHM) ranging from 6 ps (Ref. 12) to about 35 ps,[7,13–15] or even longer (≥100 ps).[16,17] Among these sources, particle beams from accelerators may be short (Linac electron bunch could be as short as 1 ps) but hard to obtain. On the other hand, laser pulses are easily available in most university laboratories. However, the lasers employed in previous studies had pulse widths too long compared to measured MCP resolutions to be neglected. The results should be considered as a convolution of the laser pulse profile and the MCP response function[18] so that, in principle, a deconvolution[19] should be involved to distinguish the contributions of the source and the detector. Even for the shortest pulse used before,[12] the pulse width (6 ps) was still significant when compared to the measured detector resolution (28 ps) and cannot be ignored. Another method to determine the MCP resolution with a 130 fs laser pulse at 400 nm has been discussed before.[20] Low-energy electrons from single ionization of Xe were selected by coincidence with Xe^+ ions as well as spatial filtering. The TOF spectra obtained by a fast time-to-analog converter (TAC) gave a resolution of 18 ps (rms). Unfortunately, this method is impossible to be implemented for detectors with no coincidence, such as ours.

Here, we demonstrate a new method for measuring the time resolution of MCP detectors with UV photons produced by a femtosecond laser. We describe our experimental setup in Sec. II. The analysis of the experimental results is presented in Sec. III. Section IV summarizes this article.

II. EXPERIMENTAL SETUP

The electron detector in our MBEES setup is a chevron MCP set with an impedance-matched anode,[21,22] manufac-

a)Electronic mail: chang@phys.ksu.edu.

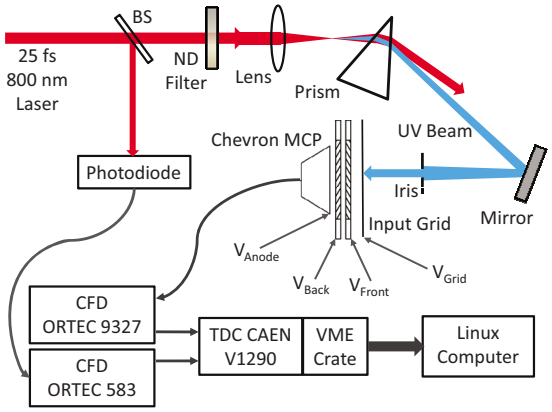

FIG. 1. (Color online) Experimental setup to measure the temporal resolution of the MCP electron detection system. Laser pulses of 25 fs at 800 nm are focused in air by a lens ($f=100$ mm) and generate UV photons at 267 nm. Part of the laser beam is reflected by a beam splitter (BS) to a photodiode. The laser intensity can be adjusted by a variable neutral density (ND) filter. A prism separates the 800 and 267 nm beams and the UV beam is reflected to the MCP detector by a mirror. The detector is housed in a vacuum chamber. Signals from the photodiode and the MCP were processed by two CFDs and sent to the TDC as the start and stop signals, respectively. A VME crate transmits the TDC data to a computer for analysis.

tured by Jordan TOF Products, Inc.[23] The impedance-matched anode provides subnanosecond rise time and reduces signal ringing as well making this detector suitable for applications in electron detection that have a desire of high temporal resolution. At the same time, an input grid provides a flat electric field in front of the MCP input surface with adjustable potential. This feature allows the electron impact energy onto the MCP to be varied to optimize the detection efficiency, which is a function of the electron energy.[21,22,24,25] The detector has an effective diameter of 40 mm, a channel diameter of $D=25$ μm, and a channel length (single MCP thickness) of $L=1$ mm so that a length-to-diameter ratio $\alpha=L/D=40$. The maximum allowed voltage across each plate is 1000 V and the gain is at least 1000 per plate at this voltage.

The bias voltages of the MCP detector are supplied by a high voltage power supply (HVPS) through a voltage divider, also provided by Jordan TOF Products, Inc. As shown in Fig. 1, the input grid of the detector is grounded ($V_{\text{grid}}=0$ V). The MCP front (V_{front}) and back (V_{back}) voltages and anode voltage (V_{anode}) are all linearly proportional to the output of the HVPS (V_{HVPS}). The MCP bias voltage is $V_{\text{MCP}}=V_{\text{back}}-V_{\text{front}}$.

Figure 1 shows a schematic of the experimental setup to measure the temporal resolution of the detector. Laser pulses of 25 fs at 800 nm from a Ti:sapphire chirped pulse amplifier system[26] with 1.5 kHz repetition rate are focused in air by a 100 mm lens. Part of the laser beam is reflected from a beam splitter to a fast photodiode which will provide the starting signal for the DAQ system. The laser intensity can be adjusted by a variable neutral density filter. As the air is ionized at the focal point of the 0.2 mJ pulses, UV light at the third order harmonic wavelength (267 nm) is produced. A prism downstream in the path separates the fundamental and UV beams and the UV beam is reflected to the MCP detector by an aluminum mirror. The detector is housed in a chamber evacuated by a turbo pump with a base pressure less than 4×10^{-6} Pa(3×10^{-8} Torr). An iris at the entrance window of the vacuum chamber was used to reduce scattered light.

Two CFDs are used to achieve the best timing output for pulses with amplitude fluctuations. The first CFD is ORTEC 583. It receives the photodiode signal and then the negative NIM output pulse goes to a 16-channel multihit TDC (CAEN V1290N) as the start signal. The MCP output is sent to an ORTEC 9327 CFD, which is capable of processing pulse widths between 250 ps and 5 ns without the need to adjust an external delay cable.[27] The negative NIM signal from the CFD 9327 is transmitted to the same TDC as the stop signal for measuring the time resolution of the whole system. The TDC has a 25 ps channel width. A LINUX computer communicates to the VME crate, which hosts the TDC, through a PCI bridge and a fiber-optic cable. At the end, a SpecTcl program[28] in the computer reads and displays spectra from the TDC in real time.

III. RESULTS AND DISCUSSION

As the MCP output is fed into the DAQ, the temporal resolution of the entire detection system can be divided into the following terms:

$$\Delta T=\sqrt{\Delta t_{\text{UV}}^2+\Delta t_{\text{MCP}}^2+\Delta t_{\text{PD}}^2+\Delta t_{9327}^2+\Delta t_{583}^2+\Delta t_{\text{jitter}}^2+\Delta t_{\text{TDC}}^2}, \quad (1)$$

where Δt_{UV} is the UV light pulse width, Δt_{MCP} is the temporal resolution of the MCP, Δt_{PD} is the timing jitter of the photodiode, Δt_{9327} and Δt_{583} are the resolutions of the CFDs 9327 and 583 where the walk and jitter are the major contributors, Δt_{jitter} is the timing jitter between two CFDs, and Δt_{TDC} is the resolution of the TDC.

The temporal resolution should be understood as the experimental uncertainty of the DAQ in the measurement of the time when an UV photon strikes the MCP, and may be represented by the FWHM of the UV peak in a photon "TOF" spectrum. The pulse width of the UV light, which is produced by the 25 fs laser, is so short that it can be treated as a delta function in time as compared with the expected MCP and DAQ resolutions (tens or hundreds of picoseconds). Therefore, it is natural to set the UV pulse width (Δt_{UV}) to zero. Similarly, since the laser pulse energy during our experiments varies less than 2%, the photodiode output amplitude is very stable and Δt_{PD} is also set to zero. At the same time, it is safe to assume the walk of the CFD (ORTEC 583) caused by the photodiode signal amplitude variation, which is the major contribution of the CFD temporal resolution, is negligible ($\Delta t_{583}\approx0$). The expression of the resolution of the system becomes $\Delta T=\sqrt{\Delta t_{\text{MCP}}^2+\Delta t_{9327}^2+\Delta t_{\text{jitter}}^2+\Delta t_{\text{TDC}}^2}$.

In order to test the resolution of the DAQ system, the photodiode signal was split and sent into both the 583 and 9327 CFDs with a time delay of a few nanoseconds. The FWHM of the TDC spectra measured in the SpecTcl program (inset in Fig. 2) contains the following terms, $\Delta t_{\text{DAQ}}=\sqrt{\Delta t_{9327,\text{PD}}^2+\Delta t_{\text{jitter}}^2+\Delta t_{\text{TDC}}^2}$. With a similar argument as shown before, the resolution of CFD 9327 ($\Delta t_{9327,\text{PD}}$) can

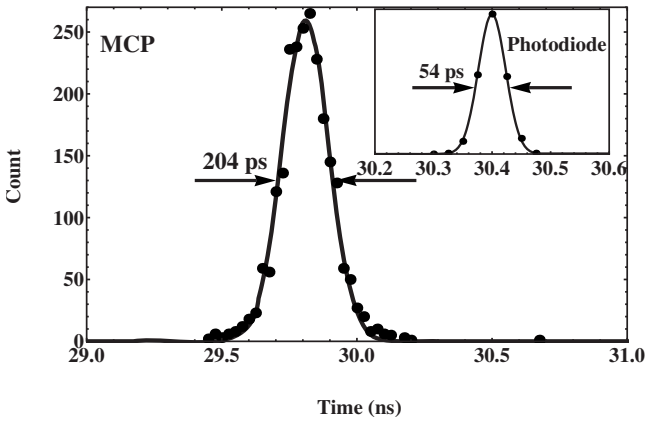

FIG. 2. UV photon TOF spectrum (dots) obtained by the setup shown in Fig. 1. The FWHM is 204 ps, obtained by fitting the experimental spectrum with a Gaussian function, $Ae^{-(t-t_0)^2/2w^2}$ (solid curve) so that ΔT(FWHM) $=2.355w$. The MCP voltage was 1800 V. The threshold of CFD 9327 was -75 mV. Inset: TDC spectrum (dots) obtained by feeding photodiode output through both 9327 and 583 CFDs. The FWHM is 54 ps, obtained by fitting the experimental spectrum with a Gaussian function (solid curve).

also be neglected in this test so that $\Delta t_{\mathrm{DAQ}}=\sqrt{\Delta t_{\mathrm{jitter}}^2+\Delta t_{\mathrm{TDC}}^2}$. The resolution of the entire detection system can then be rewritten as

$$\Delta T=\sqrt{\Delta t_{\mathrm{MCP}}^2+\Delta t_{9327}^2+\Delta t_{\mathrm{DAQ}}^2}. \tag{2}$$

The spectrum shown in the inset of Fig. 2 gives the narrowest peak ($\Delta t_{\mathrm{DAQ}}=54$ ps) obtained by adjusting the walk and external delay cable of CFD 583.

The MCP output was next sent to CFD 9327 just as shown in Fig. 1. A typical result with a FWHM of 204 ps (MCP voltage 1800 V) is shown in Fig. 2. As the MCP voltage changes from 1600 to the maximum allowed value 2000 V, an increase of the FWHM of the photon peak was observed in the spectra, shown as the circles in Fig. 3. The neutral density filter before the focusing lens (Fig. 1) was set so that the UV photon count rate within the entire range of

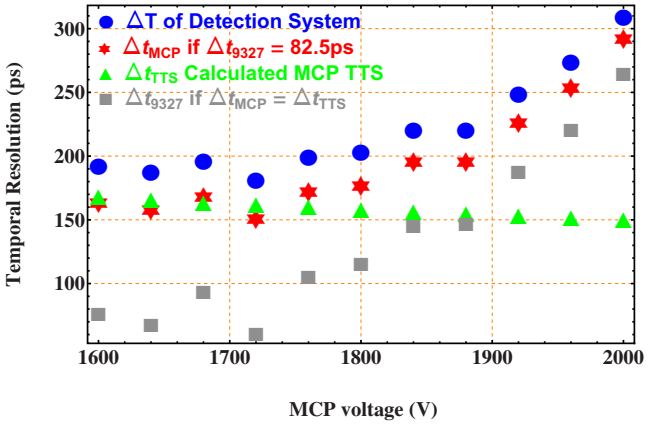

FIG. 3. (Color online) Experimentally measured FWHM of the UV photon TOF peak representing the temporal resolution of the detection system (ΔT, circles), resolution of the MCP (Δt_{MCP}, stars) calculated by Eq. (2) taking ΔT from the experiment (circles) and assuming the resolution of the CFD is $\Delta t_{9327}=82.5$ ps, transit time spread of the MCP (Δt_{TTS}, triangles) calculated by Eq. (3), and resolution of the CFD (Δt_{9327}, squares) calculated by Eq. (2) taking ΔT from the experiment (circles) and assuming the resolution of the MCP is determined by the transit time spread ($\Delta t_{\mathrm{MCP}}=\Delta t_{\mathrm{TTS}}$, triangles) as functions of MCP voltages.

the MCP voltage scan (1600–2000 V) was much lower than the laser repetition rate even with the lowest possible CFD threshold above the electronic background noises. This ensured the MCP was working in single photon detection mode (at most one photon arrives at the MCP in one laser shot). The iris was also adjusted to eliminate optical noises from scattered light. In the experiment, the threshold of the CFD was fixed at -75 mV to give a count rate of about 100 per second ($\sim$0.07 per laser shot). This produces smooth spectra within a reasonable integration time. The walk of CFD 9327 was optimized to give the narrowest peak at each MCP voltage. A similar MCP voltage scan but with varying CFD threshold to keep a flat count rate (about 70 per second) showed a similar FWHM versus voltage curve as Fig. 3. Further scans of the CFD threshold from -50 to -100 mV at several MCP voltages showed that the FWHM variation due to the change of CFD threshold was $\leq 10\%$. According to Eq. (2), either the MCP (Δt_{MCP}) or the CFD (Δt_{9327}) or both may contribute significantly to the measured FWHM of the photon peak (ΔT) since Δt_{DAQ} has been experimentally measured to be only 54 ps.

The result shown as the circles in Fig. 3 allows us to determine that our detection system should be operating at an MCP voltage of about 1800 V. Since the count rate above the CFD threshold increases as the MCP voltage increases, it is quite obvious that an MCP voltage of 1800 V is a well-balanced point giving a good temporal resolution and a high count rate at the same time.

Second, the typical walk and jitter of CFD 9327 are ± 40 and 20 ps, respectively.[27] We may take these values to be the resolution of the CFD, $\Delta t_{9327}=\sqrt{80^2+20^2}=82.5$ ps, and calculate the MCP resolution with Eq. (2), $\Delta t_{\mathrm{MCP}}=\sqrt{\Delta T^2-\Delta t_{9327}^2-\Delta t_{\mathrm{DAQ}}^2}$, taking ΔT of the detection system from the experiment (circles in Fig. 3). The result as a function of MCP voltage is shown as the stars in Fig. 3.

On the other hand, the temporal resolution of an MCP detector can be determined by the transit time spread (TTS), which can be approximated by[29–31]

$$\Delta t_{\mathrm{MCP}}=\Delta t_{\mathrm{TTS}}=\sqrt{M}\cdot L\cdot\sqrt{\frac{2m}{eV_{\mathrm{app}}}}, \tag{3}$$

where m and e are electron mass and charge, respectively, L is the length of the channel or the thickness of a single MCP, M is the number of MCPs in the assembly, and $V_{\mathrm{app}}=V_{\mathrm{MCP}}/M$ is the voltage applied on one MCP. For our chevron MCP detector, $L=1$ mm and $M=2$, and the TTS can be easily plotted as a function of the MCP voltage, shown as the triangles in Fig. 3. However, this calculation is not consistent with the MCP resolution calculated from our measurement assuming a constant CFD resolution (stars in Fig. 3). The TTS predicts better resolutions at higher voltages, but our observation shows the opposite.

A possible explanation of this inconsistency may be related to the space charge saturation in the channels of the MCP. In our UV photon detection experiments, the MCP detector was not operating in a fully saturated mode. The pulse height distribution of the MCP output is probably still a negative exponential distribution.[32] However, with a gain of 1000 per plate when the voltage is close to 2000 V, some

of the channels in the detector, especially in the second MCP, would probably be saturated. The portion of the saturated channels would be larger under higher bias voltage. The electron packet in a saturated channel moves more slowly, or equivalently, has a longer transit time than that in a nonsaturated channel. Consequently, the TTS of a partially saturated MCP detector becomes larger than either a nonsaturated or completely saturated one, due to the fact that the saturated and nonsaturated channels have different transit times. Since the resolution of the MCP calculated from the experimental results (stars in Fig. 3) at MCP voltage between 1600 and 1800 V is quite consistent with the TTS calculation (triangles), we may argue that the detector is not saturated below 1800 V. As the voltage increases beyond 1800 V, the detector enters the partially saturated mode so that the TTS increases significantly.

Alternatively, we may take the MCP resolution calculated by the TTS as is and derive the temporal resolution of the CFD from the measured FWHM of the photon peak and MCP temporal resolution by Eq. (2), $\Delta t_{9327} = \sqrt{\Delta T^2 - \Delta t_{\mathrm{MCP}}^2 - \Delta t_{\mathrm{DAQ}}^2}$. The result as a function of MCP voltage is plotted as the squares in Fig. 3. At low MCP voltages, the result is more or less consistent with the specification given by ORTEC.[27] However, as the voltage goes beyond 1750 V or so, the CFD resolution deteriorates dramatically. The factory specification was determined with a signal having a pulse width of 300 ps FWHM.[27] However, the output from our MCP detector probably has a rise time of at least 400 ps and a pulse width of more than 700 ps.[19] Therefore, it is reasonable to argue that, as the MCP voltage increases, both the amplitude and shape of the MCP output pulses change significantly so that the 9327 CFD cannot handle the signal within its 80 ps uncertainty range and the resolution degrades to over 250 ps near an MCP voltage of 2000 V. Further discussion on electronics including CFD is beyond the scope of this paper. More detailed analysis on fast timing electronics may be found elsewhere.[33,34]

In fact, the result shown in Fig. 3 is most likely due to a combination of a partially saturated MCP detector and a CFD working with signals beyond its optimum range of pulse width and shape. Although the experimental result allowed us to determine the operating point of our detection system, further tests with higher temporal resolution to quantitatively determine the contributions of the MCP and the CFD to the final temporal resolution is difficult at the present time due to a lack of proper electronic devices including a faster CFD, TAC, and/or oscilloscope.

IV. CONCLUSIONS

We presented an experiment to measure the temporal resolution of an MCP electron detector in a single-particle detection mode with UV photons produced by 25 fs Ti:sapphire laser pulses. In this way, the contribution of the photon source to the results of the measurement can be eliminated and the resolution of the detection system can be obtained without any ambiguity. This detector is one of the key components in the MBEES setup under development. The results put us one step closer to the characterization of a 25 as XUV pulse (one atomic unit of time), and demonstrated a general method to determine the time resolution of MCP-based particle detectors as well.

In the experiment, we measured the FWHM of the UV photon peak in the TOF spectrum as a function of the MCP bias voltage obtained by our electron detection system with a 40 mm diameter chevron MCP and an ORTEC 9327 CFD as the key components. The result allowed us to determine that the operating point of our detection system should be at MCP voltage of about 1800 V. At this voltage, the temporal resolution of the entire detection system including the MCP detector as well as the DAQ system is about 200 ps. In future electron detection experiments, because the yield of the secondary electrons in the first collision of the incident electrons would be higher than UV photons, the transit time spread in the MCP would be reduced.[13] For the same reason, the MCP detector would be running in a more saturated mode[32] so that the variation of the MCP output would also be reduced, resulting in a reduced walk in the CFD. Consequently, the timing uncertainties from both the MCP and CFD would be lower. Therefore, the FWHM of the UV photon peak may be regarded as the lower limit of the resolving power of our detection system. The measured temporal resolution satisfies the requirement for the MBEES setup to correctly retrieve the pulse duration of 25 as XUV pulses.[4]

The single-photon-detection resolution of the MCP was estimated to be about 180 ps FWHM. This value is consistent with theoretical calculation of TTS (Refs. 29–31) as well as measurements for chevron MCPs with channel diameters similar to ours.[7,15–17] We contribute the variation of the resolution as a function of the MCP voltage to a partially saturated MCP detector and/or a CFD working with signals beyond its optimum range of pulse width and shape.

ACKNOWLEDGMENTS

We acknowledge the technical assistance of K. Carnes, A. Rankin, S. D. Khan, and S. Gilbertson. This material is supported by the U.S. Army Research Office under Grant No. W911NF-07-1-0475, and by the Chemical Sciences, Geosciences, and Biosciences Division, U.S. Department of Energy under Grant No. DE-FG02-86ER13191.

[1] M. Hentschel, R. Kienberger, C. Spielmann, G. A. Reider, N. Milosevic, T. Brabec, P. Corkum, U. Heinzmann, M. Drescher, and F. Krausz, Nature (London) **414**, 509 (2001).
[2] G. Sansone, E. Benedetti, F. Calegari, C. Vozzi, L. Avaldi, R. Flammini, L. Poletto, P. Villoresi, C. Altucci, R. Velotta, S. Stagira, S. D. Silvestri, and M. Nisoli, Science **314**, 443 (2006).
[3] X. Feng, S. Gilbertson, H. Mashiko, H. Wang, S. D. Khan, M. Chini, Y. Wu, K. Zhao, and Z. Chang, Phys. Rev. Lett. **103**, 183901 (2009).
[4] M. Chini, H. Wang, S. D. Khan, S. Chen, and Z. Chang, Appl. Phys. Lett. **94**, 161112 (2009).
[5] P. Kruit and F. H. Read, J. Phys. E **16**, 313 (1983).
[6] K. Zhao, C. Wang, X. Feng, S. Gilbertson, S. D. Khan, and Z. Chang, *Proceedings of the Second International Conference on Attosecond Physics* (Kansas State University, Manhattan, Kansas, 2009), URL: http://jrm.phys.ksu.edu/Atto-09/.
[7] M. Akatsu, Y. Enari, K. Hayasaka, T. Hokuue, T. Iijima, K. Inami, K. Itoh, Y. Kawakami, N. Kishimoto, T. Kubota, M. Kojima, Y. Kozakai, Y. Kuriyama, T. Matsuishi, Y. Miyabayashi, T. Ohshima, N. Sato, K. Senyo, A. Sugi, S. Tokuda, M. Tomita, H. Yanase, and S. Yoshino, Nucl. Instrum. Methods Phys. Res. A **528**, 763 (2004).
[8] J. Va'vra, C. Ertley, D. W. G. S. Leith, B. Ratcliff, and J. Schwiening,

Nucl. Instrum. Methods Phys. Res. A **595**, 270 (2008).
[9] H. Brockhaus and A. Glasmachers, IEEE Trans. Nucl. Sci. **39**, 707 (1992).
[10] A. S. Tremsin, O. H. W. Siegmund, J. S. Hull, J. V. Vallerga, J. B. McPhate, J. Soderstrom, J.-W. Chiou, J. Guo, and Z. Hussain, IEEE Trans. Nucl. Sci. **54**, 706 (2007).
[11] A. S. Tremsin, G. V. Lebedev, O. H. W. Siegmund, J. V. Vallerga, J. S. Hull, J. B. McPhate, C. Jozwiak, Y. Chen, J. H. Guo, Z. X. Shen, and Z. Hussain, Nucl. Instrum. Methods Phys. Res. A **580**, 853 (2007).
[12] H. Kume, K. Koyama, K. Nakatsugawa, S. Suzuki, and D. Fatlowitz, Appl. Opt. **27**, 1170 (1988).
[13] M. Ito, H. Kume, and K. Oba, IEEE Trans. Nucl. Sci. **31**, 408 (1984).
[14] J. Va'vra, J. Benitez, D. W. G. S. Leith, G. Mazaheri, B. Ratcliff, and J. Schwiening, Nucl. Instrum. Methods Phys. Res. A **572**, 459 (2007).
[15] C. Field, T. Hadig, D. W. G. S. Leith, G. Mazaheri, B. Ratcliff, J. Schwiening, J. Uher, and J. Va'vra, Nucl. Instrum. Methods Phys. Res. A **553**, 96 (2005).
[16] B. Leskovar and C. C. Lo, IEEE Trans. Nucl. Sci. **25**, 582 (1978).
[17] C. Ertley, J. Anderson, K. Byrum, G. Drake, H. Frisch, J.-F. Genat, H. Sanders, and F. Tang, IEEE Trans. Nucl. Sci. **56**, 1042 (2009).
[18] J. P. Boutot, J. C. Delmotte, J. A. Miehé, and B. Sip, Rev. Sci. Instrum. **48**, 1405 (1977).
[19] P. Wurz and L. Gubler, Rev. Sci. Instrum. **67**, 1790 (1996).
[20] A. Vredenborg, W. G. Roeterdink, and M. H. M. Janssen, Rev. Sci. Instrum. **79**, 063108 (2008).
[21] J. L. Wiza, Nucl. Instrum. Methods **162**, 587 (1979).
[22] V. D. Dmitriev, S. M. Luk'yanov, Y. E. Penionzhkevich, and D. K. Sattarov, Instrum. Exp. Tech. **25**, 283 (1982).
[23] *Instruction Manual—40 mm MCP Microchannel Plate Detector* (Jordan TOF Products, Inc., Grass Valley, California, 2009).
[24] G. W. Fraser, Nucl. Instrum. Methods **206**, 445 (1983).
[25] *Long-Life™ Microchannel Plates* (Burle Technologies, Inc., Sturbridge, Massachusetts, 1997).
[26] B. Shan, C. Wang, and Z. Chang, U.S. Patent No. 7,050,474 (23 May 2006).
[27] *Model 9327 1-GHz Amplifier and Timing Discriminator Operating and Service Manual* (Advanced Measurement Technology, Inc., Oak Ridge, Tennessee, 2002).
[28] R. Fox, C. Bolen, K. Orji, and J. Venema, *Proceedings of the 11th Annual Tcl/Tk Conference* (New Orleans, Louisiana, 2004), http://www.tcl.tk/community/tcl2004/Papers/.
[29] J. Adams and B. W. Manley, IEEE Trans. Nucl. Sci. **13**, 88 (1966).
[30] E. H. Eberhardt, IEEE Trans. Nucl. Sci. **28**, 712 (1981).
[31] G. W. Fraser, Nucl. Instrum. Methods Phys. Res. A **291**, 595 (1990).
[32] J. L. Wiza, P. R. Henkel, and R. L. Roy, Rev. Sci. Instrum. **48**, 1217 (1977).
[33] S. Cova, M. Ghioni, and F. Zappa, Rev. Sci. Instrum. **62**, 2596 (1991).
[34] S. Cova, M. Ghioni, F. Zappa, and A. Lacaita, Rev. Sci. Instrum. **64**, 118 (1993).